To the Graduate Council:

I am submitting herewith a thesis written by Carvil Eugene Thomas Chalk entitled "Feasibility of Focusing Optics for the use of RELIEF in Engine Test Facilities." I have examined the final copy of this thesis for form and content and recommend that it be accepted in partial fulfillment of the requirements for the degree of Master of Science, with a major in Engineering Science.

L. Montgomery Smith

L. Montgomery Smith, Major Professor

We have read this thesis
and recommend its acceptance:

Dennis Keefer

Lloyd M Davis

Ronald H. Kirby

Accepted for the Council:

C W Minkel

Associate Vice Chancellor and
Dean of the Graduate School

Feasibility of Focusing Optics for the use of RELIEF in Engine Test Facilities

A Thesis
Presented for the
Master of Science
Degree
The University of Tennessee, Knoxville

Carvil Eugene Thomas Chalk
August 1996

DEDICATION

This thesis is dedicated to

my Lord and Savior, Jesus Christ

who supplied my every need

through those with whom

He surrounded me:

my wife

who has filled my life with joy;

my parents

who have guided and supported me;

my sister

who has encouraged me;

my friends

who have stood by me;

all of you

who have given freely of your lives and

have become a part of mine.

Thank you.

ACKNOWLEDGMENTS

I am grateful to several people for the opportunity to complete this work. Dr. Ronald H. Kohl has guided me with patience and understanding during these two years. His knowledge and wisdom are well appreciated. Dr. L. Montgomery Smith has served as my advisor and professor giving me insight into the world of optics, and he has served as my committee chairman. The advice and suggestions from Dr. Smith and Dr. Kohl during the final preparation of this manuscript have been invaluable. Drs. Lloyd Davis and Dennis Keefer served as the other members of my committee, and without their guidance I would not have learned all I needed to prepare this document.

I also extend my thanks to Sverdrup Technology, Inc. and the University of Tennessee Space Institute, which provided me with a graduate research assistantship. This work was conducted at Arnold Engineering Development Center, Arnold Air Force Base, Tennessee under BOA A96B-08, work order number A96W-10-Part 1, between Sverdrup Technology, Inc. and The University of Tennessee.

Additionally, I would like to thank Mr. David Manzi and Ms. Shelley Merrill of Specialty Optics Manufacturing & Design, Inc. They provided valuable information used in simulating manufactured optics.

Finally, the greatest appreciation goes to my family. To my wife, Jacqueline, and to my father, mother and sister, I am grateful for the love and support they have given to me. Without them I could not have accomplished all that I have during the course of my graduate studies.

ABSTRACT

Trial lens systems of focusing optics were designed and analyzed for their effectiveness in focusing and co-locating two tagging laser beams to be used in the technique of Raman Excitation and Laser Induced Electronic Fluorescence (RELIEF). The RELIEF technique is being developed to provide a measurement of local flow velocities of engine-inlet flows in engine test facilities. The engine test cells at Arnold Engineering Development Center (AEDC) served as a model around which to design the systems. The two laser beams, each containing both wavelengths of light required for Raman excitation, are equally displaced about the optic axis. The lens systems were designed to bring these two off-axis beams to a common focus at the points along a radial line extending from the center of a given engine-inlet air supply duct to near the inner surface of a cylindrical duct access window, the curvature of which matched that of the interior of the given duct. The optic axis of the trial lens systems is oriented perpendicular to, and intersects, the longitudinal axis of the duct. The two beams are contained in the plane defined by the two axes and, thus, cross within this plane.

The trial lens system designs were obtained using the Zemax™ optical design program. This program provides a platform to simulate the representative duct sizes in the engine test facilities at AEDC and to design scaled optics for each. Though Zemax™ offers the capability to optimize and analyze lens systems for use by Gaussian beams, it is limited to a rotationally symmetric case. The off-axis nature of the two laser beams and the cylindrical window used for optical access into the engine-inlet duct clearly violate

this restriction. Thus, the systems in Zemax™ were designed, optimized and toleranced strictly based on ray approximations of the off-axis beams. To analyze the Gaussian beam focusing properties of the trial lens systems, it was necessary to develop a FORTRAN code as part of this thesis.

The FORTRAN code uses a basic ray-tracing algorithm for the chief ray of each laser beam combined with a method for determining the ABCD matrices encountered by that off-axis beam. These ABCD matrix values are then used to transform the input beam using the ABCD transformation law. A limited validation of the FORTRAN code was accomplished by comparing output beam spot sizes for rotationally symmetric systems to those predicted by Zemax™. This validation showed a maximum difference of 5% between the FORTRAN code and Zemax™.

Variants of the trial lens system designs that modeled manufactured optics were simulated using a Monte Carlo technique in Zemax™. These models, along with the optimized designs for each of the trial lens systems, were analyzed using the FORTRAN code. The results showed that the designs were capable of focusing the two off-axis laser beams to the spot radii necessary to achieve RELIEF tagging (50 μm). Thus, the feasibility of these optics was quantitatively demonstrated for the optimized systems and for the models of manufactured systems.

TABLE OF CONTENTS

LIST OF TABLES

TABLE PAGE

LIST OF FIGURES

Chapter 1

Introduction

Intrusive mechanical or optical techniques that have inherent drawbacks limit high-accuracy measurement of the local flow velocities of engine-inlet flows. Hot-wire anemometers and Pitot tubes require the insertion of mechanical devices that distort the flow and present a foreign-object danger to an engine downstream. Optical techniques such as laser Doppler velocimetry and resonance Doppler velocimetry require seeding the flow with particles or trace gases, a requirement that is often undesirable. Also, they require a very steady flow with long averaging times per measurement in an attempt to obtain high precision.

Raman Excitation and Laser-Induced Electronic Fluorescence (RELIEF)[1] is a technique being developed to provide a non-intrusive, more accurate measurement of the vector velocity-profile of the airflow delivered to a jet engine under test. To obtain the vector velocity at a location in the flow, a frequency-doubled Nd:YAG laser tags the flow at that location by exciting a small volume of oxygen molecules using stimulated Raman excitation. The flow carries this excited volume for a small, specified time interval. An argon fluoride laser then interrogates this excited volume by causing it to fluoresce using laser-induced electronic fluorescence. A system of imaging optics combined with a detector array images the volume from two directions during its tagging and fluorescence, and these real-time images allow a calculation of the vector distance the volume has traveled. The vector velocity measured is the vector distance traveled divided by the time interval.

Current RELIEF techniques rely on tagging a line perpendicular to the direction of a known flow to deduce the flow velocity (See Figure 1)*. The RELIEF technique accomplishes the tagging along the length of the focused region of the laser beam. For the RELIEF technique to be used in determining the three-dimensional vector velocity of a flow, a point in that flow must be tagged.[1] Tagging two lines that cross at the desired location accomplishes marking a point in the flow. This mark is made by focusing and co-locating two laser beams, which are equally displaced about the optical axis of a set of optics, in the focal plane of these optics (See Figure 2).

RELIEF tagging, being a stimulated Raman process, is very sensitive to achieving a tight focus. Furthermore, each of the RELIEF tagging beams consists of two wavelengths: 532 nm in the green and 580 nm in the orange. The windows used for optical access into the engine-inlet duct of an engine under test must be curved to match the interior surface of the duct. The issue addressed in this thesis is the feasibility of implementation of variable-focus optics that will adequately focus the RELIEF tagging beams to all crossing points along a radial line from the center of the duct to near the inner edge of the access window.

The approach used to design the optics was to develop systems for use in a wide range of engine test facilities (up to 3.7 m in diameter) at Arnold Engineering Development Center (AEDC). This should make such systems usable almost anywhere.

---

* All figures are contained in Appendix A, Figures, and are numbered sequentially.

The constraints imposed on the optical designs were taken from the physical environment of the test facilities and the energy density required to achieve tagging. Current RELIEF techniques have been demonstrated to tag with ~130 GW/cm^2 using 100 mJ of energy per 10 ns pulse with a spot radius of 50 μm.[2] According to the developers of RELIEF, the energy distribution is approximately two-thirds green and one-third orange. The physical environment of the engine test cells has limited space outside the inlet duct in which to place the focusing optics. Thus, the approach to designing these optics was to minimize the spot radius of each beam at the crossing point to 50 μm or less and to constrain the overall length of the optics, including the movement necessary to focus along a radial line of the duct. A value of one half the duct radius or less was initially chosen as a representative maximum for the overall length. This value would eventually be relaxed to 65% of the duct radius in order to obtain co-location of the off-axis beams, to account for the presence of mirrors used to direct the beams into the duct for the folded configuration, and to ensure the optics were well separated from the outer edge of the duct for the folded configurations discussed later in Chapter 3.

The Zemax™ optical design program and a FORTRAN code, which was developed in this thesis, were used to obtain the design, tolerancing and performance of trial lens systems. Each trial lens system was obtained using the Zemax™ optical design program. The spot size and co-location of ray approximations to the laser beams were optimized at the RELIEF focus points by using a Zemax™ optimization routine. (Ray approximations to the beams were employed since Zemax can only treat Gaussian beams in rotationally symmetric systems. The off-axis nature of the beams and the cylindrical window used for optical access into the duct clearly violate this restriction.) The FORTRAN code was used to calculate the Gaussian beam spot radius for each of the off-axis beams. The code employed a basic ray tracing algorithm for the central ray of each wavelength component of each off-axis beam, combined with the calculation of the ABCD matrices of the optics as encountered by each off-axis beam.

Chapter 2 describes the principles of RELIEF and the application of ABCD matrix theory to ray-tracing and Gaussian beam propagation. Chapter 3 outlines the design process using Zemax and the development of the FORTRAN code. Chapter 4 gives the optimal system designs obtained, a limited validation of the FORTRAN code, and the focus spot radius results. Chapter 5 concludes with a discussion of the results, further considerations for future applications of the methodology and analysis presented in this thesis, and the implications for RELIEF.

Chapter 2

Background

Principles of RELIEF

RELIEF is a technique that can be used for the non-intrusive, highly accurate measurement of nearly instantaneous, local flow velocities.[1-6] The flow is tagged by exciting a small volume of oxygen molecules using stimulated Raman excitation. Once this excited volume is carried with the flow for a small, specified time interval, it is induced to fluoresce (interrogated) using laser-induced electronic fluorescence. The small volume is imaged during its tagging and fluorescence, and from this the distance the volume has traveled is known. The velocity can be calculated using the fundamental definition $\Delta x/\Delta t$, and, if the time interval is small enough, the calculated velocity can be considered instantaneous.

Oxygen molecules in the flow are tagged by excitation to the first vibrational state of the ground electronic state by stimulated Raman excitation.[1] Two co-located laser beams, each containing two wavelengths separated by the energy difference between the ground state and the first vibrational state, accomplish the tagging. The wavelengths of 532 nm and 580 nm are used since the separation between them is 1555 cm^{-1} in frequency, the required energy difference.[1] The 532 nm wavelength is generated using a frequency-doubled, Q-switched Nd:YAG laser and is focused into a high pressure O_2 cell that converts some of the incident radiation to the 580 nm wavelength by the process of stimulated vibrational Raman scattering.[3]

Interrogation of the tagged oxygen molecules is accomplished through laser-induced electronic fluorescence. [1] This process uses an argon fluoride laser operating near 193 nm to excite one rotational sublevel of the first vibrational, or v′=1, level to the v′=7 level. (This excitation occurs only for the tagged oxygen molecules that are in the vibrationally excited level. In turbine engine test flows, the other oxygen molecules will remain in the ground vibrational level.) The excited population in the v′=7 level instantaneously transitions into a dissociating electronic state of the same energy level. The fluorescence of the molecules results from the molecular fraction in this state that emits prior to complete dissociation and occurs in near UV and visible wavelengths (200 nm - 400 nm). [4] The emission time is nearly instantaneous due to rapid dissociation; thus, the interrogation time is on the order of the pulse duration, approximately 10 ns. [4]

Imaging of the volume is achieved using a gated, intensified, UV sensitive CID camera. This image is analyzed by a computer to locate the tagged spots. [1] Currently this analysis is done off-line. In the engine test application being developed, this will be done in real time. The time interval between tagging and interrogation is currently one to two microseconds; however, in the dry air of engine test facilities this is expected to be 20 to 100 microseconds (for ~30% relative humidity or less)[2].

ABCD Matrix Theory

As shown by Siegman[7] and his predecessors, 2×2 ABCD matrices describe the propagation of geometrical rays through many types of optical elements and systems so long as the optical beam meets the paraxial approximation. As defined by Siegman[7], an optical beam whose plane wave components travel at angles less than thirty degrees with respect to the optical axis is considered paraxial. Numerous optical elements can be described by general forms of these matrix equations such that

$$x' = Ax + B\alpha , \tag{1}$$

$$\alpha' = Cx + D\alpha , \tag{2}$$

where x is the ray displacement from optic axis and α is the index-weighted ray slope with respect to the optic axis defined by

$$\alpha = n(z)\frac{dx(z)}{dz}, \tag{3}$$

where $n(z)$ is the index of refraction of the medium at longitudinal position z.[7] These equations can be more easily written in matrix form as

$$\begin{bmatrix} x' \\ \alpha' \end{bmatrix} = \begin{bmatrix} A & B \\ C & D \end{bmatrix} \begin{bmatrix} x \\ \alpha \end{bmatrix} \tag{4}$$

where the primed quantities are the corresponding values at the output plane. (See Figure 3.)

For example, if a ray in a medium with index of refraction n is traveling in the z-direction with displacement x and slope α with respect to the optic axis at some input plane z_1 (See Figure 4), then after emerging at a plane z_2 a distance s along the axis, the ray will have a new displacement x' and slope α' given by

$$x' = x + s\alpha \tag{5}$$

$$\alpha' = \alpha , \tag{6}$$

and the corresponding ABCD matrix, M, is given by

$$M = \begin{bmatrix} 1 & \frac{s}{n} \\ 0 & 1 \end{bmatrix}. \tag{7}$$

If this same ray passes through a thin lens of focal length f (See Figure 5), then the output quantities are given by

$$x' = x, \tag{8}$$

$$\alpha' = -\frac{1}{f}x + \alpha, \tag{9}$$

and

$$M = \begin{bmatrix} 1 & 0 \\ \frac{-1}{f} & 1 \end{bmatrix}.$$

Thus, in each case, the ray is transformed linearly by the element, and the 2 × 2 ABCD matrix completely describes the effect of the optical element on the ray. Additionally, by using the definition of α given above (eq. 3), Snell's law of refraction is included in the ABCD transformations, and the value of the matrix determinant is always[7]

$$AD - BC = 1. \tag{10}$$

Another property of matrix theory useful to optics is the ability to cascade the matrices of several elements to determine a system matrix. If we define

$\vec{x}_0 = \begin{bmatrix} x \\ \alpha \end{bmatrix}$ for an input ray, and $M_1 = \begin{bmatrix} A & B \\ C & D \end{bmatrix}$ for the first optical element, then

$$\vec{x}_1 = M_1 \vec{x}_0. \tag{11}$$

If the ray propagates through another element M_2, then

$$\vec{x}_2 = M_2\vec{x}_1 = M_2 M_1\vec{x}_0 . \qquad (12)$$

This pattern can be repeated for *n* elements such that

$$\vec{x}_n = M_{Total}\vec{x}_0 , \qquad (13)$$

where

$$M_{Total} = M_n\, M_{n-1}\ldots M_1 . \qquad (14)$$

Thus, the propagation of a ray can be done step by step, or the system matrix can be calculated and the transformation completed in one step. Though the results to this point have been derived for the rays associated with plane waves, the rays associated with spherical waves can also be treated using the ABCD matrix values.

If a point source on the optic axis radiates spherical waves from $z = 0$, then at a plane $z = R(z)$ each ray has a slope defined as

$$\alpha(z) = n(z)\frac{dx}{dz} = n(z)\frac{x}{R(z)}, \qquad (15)$$

and

$$R(z) = \frac{n(z)x}{\alpha}. \qquad (16)$$

(See Figure 6.)

Therefore, a ray associated with a spherical wavefront is transformed by an ABCD element or system such that the output is given by

$$\frac{R_2}{n_2} = \frac{x'}{\alpha'} = \frac{Ax + B\alpha}{Cx + D\alpha}, \qquad (17)$$

which can be obtained from the fundamental definition of the of ABCD matrices (eqs.1 & 2).

In addition to describing the propagation of plane and spherical waves of geometric optics, ABCD matrices can transform paraxial Gaussian beams through orthogonal systems. (A system containing non-rotationally symmetric components is orthogonal if the principal axes of the components are aligned. [7]) At the input plane $z = z_1$ of an arbitrarily complex, orthogonal optical system, consider a Gaussian beam with a field component envelope in the x-direction of the form

$$\tilde{u}_1(x_1) = \exp[-j\frac{\pi x_1^2}{\tilde{q}_1\lambda_1}], \tag{18}$$

where

$$\frac{1}{\tilde{q}_1} = \frac{1}{R_1} - j\frac{\lambda_1}{\pi\omega_1^2}. \tag{19}$$

That is, at the input location z_1, u_1 is one transverse component of the field component envelope, λ_1 is the wavelength in the medium, R_1 is the phase curvature, and ω_1 is the spot size. In this case, at the output plane $z = z_2$, the generalized one-dimensional Huygen's integral gives

$$\tilde{u}_2(x_2) = \sqrt{\frac{1}{A + n_1B/\tilde{q}_1}}\exp\left[-j\frac{\pi x_2^2}{\tilde{q}_2\lambda_2}\right], \tag{20}$$

where the complex q-parameter has been transformed by

$$\frac{\tilde{q}_2}{n_2} = \frac{A(\tilde{q}_1/n_1) + B}{C(\tilde{q}_1/n_1) + D}, \tag{21}$$

the same equation as for a spherical wave in geometric optics.[7] Thus, given the input parameters R_1 and ω_1 of a Gaussian beam, along both orthogonal axes, the output values R_2 and ω_2 along each orthogonal axis can be calculated by matching the real and imaginary components of the complex q-parameter for each orthogonal component of the wave. This transformation requires knowledge of the ABCD matrix values to be used. The equations needed to obtain these matrix values for a Gaussian beam have been derived by Massey and Siegman.[8]

In the derivation of the ABCD matrices for the refraction and reflection of a Gaussian beam at a tilted, ellipsoidal surface, Massey and Siegman[8] used a phase matching argument for the transverse phase and amplitude variations at the surface boundary. Using a complex wave of the form

$$\tilde{u}_i = \tilde{A}_i \exp\left(-j\phi_i\left[x_i, y_i, z_i\right]\right), \tag{22}$$

where the complex phase is defined as

$$\phi_i = k_i z_i + \frac{k_i}{2}\left(\frac{x_i^{\,2}}{q_{Ti}} + \frac{y_i^{\,2}}{q_{Si}}\right) \tag{23}$$

and the component variables in the complex phase are given by

$$k_i = \frac{2\pi n_i}{\lambda_0} \quad \text{and} \quad \frac{1}{q_i} \equiv \frac{1}{R_i} - j\frac{\lambda_0}{\pi n_i \omega_i^{\,2}}, \tag{24}$$

where R_i is the phase curvature of the Gaussian beam, Massey and Siegman[8] derived ABCD matrix equations for reflection and refraction in both the tangential (T) and sagittal (S) planes at a surface. These results were later modified by Siegman[7] for use as matrices whose determinants met the requirement of equation (10), so that the q-

parameters in the tangential and sagittal planes at an interface would obey equation (21). The results showed that a Gaussian beam is refracted in the tangential and sagittal planes as given by the matrices

$$\mathrm{M}_{\mathrm{Tangential}} = \begin{bmatrix} \dfrac{\cos\theta_2}{\cos\theta_1} & 0 \\ \dfrac{\Delta n_e}{R_T \cos\theta_1 \cos\theta_2} & \dfrac{\cos\theta_1}{\cos\theta_2} \end{bmatrix} \tag{25}$$

$$\mathrm{M}_{\mathrm{Sagittal}} = \begin{bmatrix} 1 & 0 \\ \dfrac{\Delta n_e}{R_S} & 1 \end{bmatrix} \tag{26}$$

where

$$\Delta n_e = n_2 \cos\theta_2 - n_1 \cos\theta_1, \tag{27}$$

and Snell's law

$$n_1 \sin\theta_1 = n_2 \sin\theta_2 \tag{28}$$

holds. Not to be confused with equation (24), R_T and R_S refer to the appropriate surface radius of curvature. Reflection at an ellipsoidal surface is given by the matrices

$$\mathrm{M}_{\mathrm{Tangential}} = \begin{bmatrix} 1 & 0 \\ \dfrac{2}{R_T \cos\theta} & 1 \end{bmatrix}, \tag{29}$$

$$\mathrm{M}_{\mathrm{Sagittal}} = \begin{bmatrix} 1 & 0 \\ \dfrac{2\cos\theta}{R_S} & 1 \end{bmatrix}. \tag{30}$$

(Note: For a flat mirror, both reflection matrices reduce to the identity matrix.) Given n_1 and n_2, these equations depend only on the incident angle θ_1 of the chief (or central) ray in the tangential plane and the radius of curvature R_T or R_S of the surface in the sagittal or tangential plane. Thus, with these three variables known, it is possible to propagate a Gaussian beam through an arbitrarily complex, orthogonal optical system in the method described earlier in this section using these matrices and the ABCD translation matrix given by equation (7). This capability was used in the development of the FORTRAN code and is described later in Chapter 3.

Non-Paraxial Ray Tracing

Non-paraxial ray tracing techniques provide a method for following the path of a ray, or rays, through complex optical systems without a loss of accuracy for rays that do not lie near the optic axis nor travel at sufficiently shallow angles such that the paraxial approximation of $\sin\theta \approx \theta$ holds true, where θ, in this case, is the angle that the ray makes with the optic axis.[9] These techniques rely on the same type of transformation as the rays in ABCD matrix theory; however, the transformations are not always linear because the update matrices used to calculate displacement and slope contain coefficients which are generally functions of displacement and slope.[9] Another advantage of non-paraxial ray tracing is its use of rays that can have different slopes and displacements along orthogonal axes. This allows treatment of systems containing astigmatic elements such as cylindrical lenses or windows so long as the principle curvatures of these surfaces are located in common planes throughout the system.

The basic premise of non-paraxial ray tracing is a combination of repeated sequences of translation and refraction followed by a final translation to the output plane, as shown by Smith.[9] Given the repetitive nature of the calculations, and the complexity of most non-trivial optical systems, they are better implemented in a computer code. The equations for the variables used in the update equations of the code must be derived for each type of surface encountered by the beam.

In a technique developed by Smith[9], a series of update equations for translation to and refraction by spherical interfaces are derived. These equations update the x and y positions as

$$x' = x + B\alpha \tag{31}$$

$$y' = y + B\beta \tag{32}$$

where

$$B = z / n\cos\theta . \tag{33}$$

The values for z are given by solving for the translation distance to a sphere in terms of x' and y', and θ is a function of α, β and n as shown in Figure 7. The refraction equations update the slope as

$$\alpha' = Cx + \alpha \tag{34}$$

$$\beta' = Cy + \beta \tag{35}$$

where C is derived by equating components in a vector formulation of Snell's law at a spherical interface.

The fundamental sequence of events is to input initial slopes and displacements, propagate the ray to the first surface, update its position, refract it through the surface and update the slope. This translation-refraction process is repeated for each subsequent surface until the final surface is reached. A final translation to the image plane is then calculated, and the positions at the output plane are the last updated. This process, with modifications and additions developed in this thesis to treat cylindrical and planar surfaces, was used in the development of the FORTRAN code and is discussed in the section on code development in Chapter 3.

Chapter 3

Design, Synthesis, and Analysis

Trial lens systems were designed, and manufactured lens systems were then modeled and tested to investigate the feasibility of focusing optics for the use of RELIEF in engine test facilities. Engine test cells at Arnold Engineering Development Center (AEDC) were used as a model for development. The engine-inlet ducts at AEDC in which measurements are desired, have five representative diameters: 4 inches (101.6 mm), 1 foot (304.8 mm), 3 feet (914.4 mm), 6 feet (1,828.8 mm), and 12 feet (3,657.6 mm). The four inch diameter is characteristic of the interior flows of accurate aircraft models from which the engine inlet flows are obtained under the many flight conditions of interest. The other diameters are characteristic of the engine inlet ducts that supply the airflow to engines under test. Each such duct requires a scaled set of optics and input laser beam radii in order to obtain adequate performance. Both the test cell environment and the RELIEF technique provide non-trivial requirements and conditions that have to be met by the trial lens systems during the design process.

Requirements and Conditions

In order for the focusing optics to fit within the test cells, the size and the length of the optical focusing systems must be limited. The diameter of the optics is established by the requirement that the initial off-axis beams incident on the lenses cross in the focal plane at a large enough angle to form a suitable point. This diameter is about one-twelfth the duct radius. The overall length of the system is constrained so that it will fit into the surrounding cell; a length of approximately one-half the radius of the duct was initially chosen as a representative maximum. This length does not include the additional optics or mirrors necessary to direct the incoming beams into these focusing optics.

Two orientations of the focusing optics were designed for use in the test cells. The first, referred to as in-line, placed the focusing optics perpendicular to the flow axis of the duct (See Figure 8). In this orientation, it is imperative that the length of the optics be constrained. The second orientation, referred to as folded, placed the focusing optics parallel to the flow axis of the duct, and employed a fold mirror to direct the beams through the window and into the duct (See Figure 9). This second configuration was developed in the event that the constraints applied to the inline configuration still resulted in a system that would not fit inside the given test cell. (Note: The overall length constraint discussed earlier was relaxed to .65 times the duct radius for most of the inline configurations of the trial lens systems during the design process to achieve co-location of the two beams and is discussed later in this chapter. The overall length of the folded configurations was also relaxed to account for the presence of a fold mirror, which directs the beams into the duct, and to ensure that the optics were well separated from the outer edge of the duct.) In each case, the optic axis, the two off-axis beams, and the longitudinal axis of the duct remain coplanar.

The beam spot radius at the crossing point in the focal plane has to be small enough that the tagging laser can generate the necessary energy density to tag the flow.[2]

RELIEF has been demonstrated to require an intensity of ~130 GW/cm^2 in order to tag oxygen. This can be achieved using a focused spot radius of 50 μm and a corresponding energy of 100 mJ in a 10 ns pulse.[2] According to the developers of RELIEF, the energy distribution between the wavelengths in each beam is approximately two-thirds green and one-third orange. As this is the energy expected to be available in a RELIEF system in an engine test cell, the goal was a focused spot radius of 50 μm or less at locations along the duct radius ranging from about one-half inch inside the duct surface to the center of the duct.

Development of the Trial Lens Systems

The Zemax™-EE optical design package (referred to as Zemax through the rest of this text), version 2.9 for DOS, was initially used as the platform for the design and optimization of trial lens systems for the use of RELIEF. Later, following development of the trial lens system designs, the Zemax software was upgraded to version 4.5 for Windows™. Version 4.5 was used during and after the tolerance analysis of the designs.

Zemax is a ray tracing program that allows the user to input data on all aspects of a lens system design. The requirements on the optics were incorporated into Zemax, and separate systems were designed for each duct for both inline and folded optics. The approach taken was to develop optical systems for which the root-mean-square, ray-traced spot size about the chief ray was a minimum. As stated earlier, ray approximations to the laser beams were used since Zemax is unable to treat Gaussian beams in non-rotationally symmetric systems.

So that the traced rays would pass through the same portion of the optical system as would the input laser beams, the object distance was initially set to infinity. To test the sensitivity of the performance of the optical systems to the location of the waist of the incoming beams, the situation was also considered where the incident beam had propagated three meters from its waist before entering the optics. Obtaining rays that might follow the path of such a beam was achieved by calculating the phase curvature of the beam and setting the object distance to that value. (The two waist locations resulted in comparable system performance.) The input size of the beam was established by defining the entrance pupil diameter to be twice that of the desired input beam spot radius.

The requirement to focus the beams at locations from the center to near the edge of each duct was met using a multi-configuration optimization technique. In Zemax, the optics system was decentered with respect to the input beam for each of four configurations. Since two beams were to propagate off-axis through the system for each focusing distance, the decentration was set for positive and negative values for each of the two extremes of the range of focusing distances. The amount of decentration was determined by assuming a beam radius scaled for the given system and decentering the ray approximation to the input beams such that the wings of the corresponding Gaussian beams would not experience any significant aperturing effects due to the lens edges.

The far focus position, established for focusing at the center of the duct, was set to the duct's radius. The near focus position was set to a distance of 3.16 mm from the window assuming a tagging laser beam could be focused to a spot size of 12.5 μm. This size spot would only require 6.25 mJ of energy to achieve RELIEF tagging, and the energy level at the window would be low enough to avoid breakdown. However, if a focused spot of 12.5 μm could not be achieved at this focus position, it might still be possible to achieve a larger focused spot useful for RELIEF tagging at a distance further away from the window. The spot would be located further away from the window since an energy increase would be required to achieve RELIEF tagging using a larger spot. Thus, four configurations were considered, near focus and far focus for beams entering on both sides of the optics. Once these configurations were set, it was necessary to establish a merit function by which Zemax could optimize the variables in the system to meet the established criteria.

An empirical check showed that considering only the extreme focusing conditions during optimization would still result in achievable RELIEF focusing at locations between the far and near focus positions. This empirical check was accomplished by using a trial lens system, which was optimized as discussed below. The intermediate focusing positions, for which the two off-axis beams crossed, were correlated with the movement of the first lens element. The spot sizes at these intermediate locations were found to be appropriately sized with respect to the focused spots at the extreme focus positions. The intermediate focused spot sizes lay within the range of spot sizes established by the extremes.

Zemax offers several default merit functions with which to optimize a given lens design; however, the requirements for the optics systems in question did not lend themselves to use of one of these default merit functions. For this reason, a user-defined merit function was created using the goals of minimization of the spot radius and the co-location of the two off-axis beams in each of the two extreme focal planes.

The user-defined merit function was created using operands from Zemax. The RSCH (RMS spot size chief ray) operand was chosen to minimize the beam spot radius at the focal planes. This operand invokes a Gaussian quadrature method to estimate the spot radius of the beam with respect to the chief ray at a specified focal plane in root-mean-square (RMS) fashion.[10] The chief ray of the beam in Zemax is a ray that travels from a defined object location through the center of the entrance pupil.[10] In this system, the chief ray of each beam in Zemax corresponded to the central ray of each Gaussian beam of the tag laser. Note that the central ray of a Gaussian beam follows the same path as that of a corresponding geometrical optics ray[11].

The REAX (Real ray x-coordinate) and DIFF (difference) operands were chosen to achieve crossing of the off-axis beams in the focal planes. The REAX operand calculated the x-coordinate of a real ray traced to a given surface, in this case the image plane. REAX operands were established for both wavelengths of the laser beam in each configuration, and the target for the x-coordinate of the ray was set to zero (the optic axis of the optics system). The weight of this operand in the merit function was also set to zero, such that it had no effect on the optimization. Instead, the DIFF operand, which calculates the difference between two specified operand values, was used in each configuration to insure that both beams crossed in the image plane. Since the *x*-location was not as important as the co-location of the beams, the actual *x*-coordinate in the focal plane was not specified; rather the difference in *x*-locations of both beams was targeted to be zero (i.e., left and right beams co-located for each focus position). This method was chosen since manufactured optics are not likely to contain the symmetry necessary to focus exactly on the optic axis. With the boundary conditions established and the merit function defined, the next step in the development process was to determine a suitable initial system from which to proceed.

Since most optical systems have been designed to work with aperture filling beams that are centered on the optical axis rather than with small beams passing off-axis, locating an example optical system from which to begin development proved difficult.[12-15] However, in principle, the desired effect of the optics was found to be similar to the operation of a Galilean telescope or inverse Galilean beam expander. These optical instruments take collimated input light at one diameter and produce collimated output light at a smaller or larger diameter. Each of the instruments uses two optic elements, one positive (converging) and one negative (diverging). Thus, the basic set-up of a positive element followed by a negative element (either of which may change sign under the design optimization) was chosen as the initial design from which to begin (See Figure 10). It should be noted that two optical elements are the minimum number required to achieve variable-focus optics.

Though all the final design requirements were used in the design process, it was more feasible to proceed by starting with as few restrictions as possible on the optimization routine. Narrowing the range of selection by introducing requirements as progress was made allowed more freedom to reach an optimal design. Initially, silica was selected as the glass type for the optics and the window.

The variables chosen for optimization were the radii of curvature of the surfaces of the lenses, the center thickness of each of the lenses and the allowed movement of the positive lens element. The negative lens element remains fixed while the positive element moves to vary the focus. In the far focus position the positive is at its closest point to the negative element, and in the near focus position the positive element is at its farthest position from the negative element. The optimization routine was allowed to modify these parameters to minimize the value of the merit function so long as the parameters remained within the established boundary conditions and within physical requirements (i.e. no negative center thickness or surfaces that invaded one another). If the parameters violated these conditions, they were set to the minimum or maximum allowed value accordingly.

The two wavelengths used in each beam for RELIEF tagging resulted in the need for achromatic doublets in order to focus the two wavelengths to the same location and to the same size. With a desire to develop a design that could use stock lenses, the Melles Griot lens database contained in Zemax was referenced. An achromatic doublet from the LAO series was chosen to closely match the focal length required of the positive element for each of the trial lens systems being designed. No stock negative doublets were available; so one was created to match the required focal length. The glasses in these two doublets were each arranged in the same order with the crown glass toward the incoming beam and the flint glass facing the window of the duct (See Figure 11).

The Coddington shape and position factors suggest the opposite glass order in the second achromat. According to this convention, it is most common for the flint glass element's higher radius of curvature to face the infinite conjugate, i.e. face the incoming beams. For these trial lens system designs, the result would be that the orientation of the second achromat would be opposite to the current configuration. This conventional orientation was checked; however, neither co-location of wavelengths, nor the beams, could be achieved. For example, in a design for the one foot diameter duct with this glass orientation, the two wavelengths in each beam were separated in both the far and near focal planes by approximately nineteen microns, as were the beams themselves. As stated earlier, co-location of the wavelengths and co-location of the two beams are required for stimulated Raman excitation; thus, optimization proceeded with the crown glass of each element toward the incoming beams.

Subsequent optimization showed a continued need for variation of the positive doublet's characteristics. Thus, a design that would focus the off-axis beams to small spot radii and to the same location in image space required customized positive and negative achromatic doublets.

In an attempt to locate a supplier of cemented, negative doublets, it became apparent that it would be necessary to have these parts specially fabricated. A potential manufacturer, Specialty Optics Manufacturing and Design, Inc., was contacted to determine the best method for designing the needed parts. In terms of manufacturing and design it was decided that the two component lenses of the achromats should be air-spaced rather than cemented. This technique would allow better control of the performance after manufacturing, and it would eliminate the need to select a cement appropriate for this application. Upon further investigation into the cements used in most stock achromats, temperature limitations were discovered and proved to be incompatible with use in the engine test facilities. In general, the cement used to bond the two components of an achromatic doublet has a temperature limitation of approximately 150^{0}C or less.[15-16] The engine test cell environment can reach temperatures of up to 340^{0}C. With this information it became necessary to redesign the beam focusing systems with both the positive and negative elements as air-spaced doublets.

The earlier system design of two cemented achromats was used as the baseline for the air-spaced achromats. Essentially the achromats were separated into two components, one of crown glass and one of flint with a small air space separating them. The Schott glasses SSKN8 (crown) and SF8 (flint) were selected for the achromats upon the recommendation of design engineers at Specialty Optics. Other combinations of crown and flints were considered empirically before contacting the engineers at Specialty Optics. The combinations considered were those found in the stock achromats in the Melles Griot catalog. However, no significant change in performance was noted for these other combinations. The window remained silica.

The optimization procedure for this design was similar to prior optimizations except the curvatures toward the air space in each achromat were not required to be the same, and the air gap between the components of the two doublets could also be used as an optimization variable. In obtaining the near and far focuses, the two components forming each achromat were constrained to move together with a constant, yet optimized spacing.

Optimization of these designs was accomplished using the same merit function discussed earlier. The number of surfaces involved created a situation in which the optimization routine would frequently select unrealistic values if all the parameters were allowed to vary at once. Therefore, the parameters available for optimization were allowed to vary in turn: first, radii of curvature, followed by element thicknesses, then element travel distances, and finally the air spacing between the components of each achromatic doublet. (As mentioned earlier, the restriction on the overall length of the system was relaxed approximately 15% from the initial value of one-half the duct radius to achieve beam co-location.)

The radii of curvature were set to correspond to the optimized values obtained earlier. The thicknesses of the individual components, which have little effect on the minimum aberrations achievable, were set to values similar to those of stock lenses of the same diameter and focal length (positive or negative).[15-16] Element travel distances and element locations were also set to the maximum or minimum allowed values in order to obtain the best use of the two doublets. The air space between each component of the two doublets was set at the minimum separation to avoid edge contact or to one-half millimeter, whichever was greater. Additionally, for the folded configurations for each duct size, a minimum separation distance from the window was established to account for the presence of the fold mirror and to ensure that the optics were well separated from the outer surface of the duct. Each parameter was then optimized in turn from these initial settings. The next step in the design process was to match the optimized lens radii of curvature to test plates that could be manufactured.

Specialty Optics Manufacturing and Design, Inc. provided a list of test plates available for both positive and negative values of the radius of curvature.[17] The optimized radii of curvature were then each changed to the closest radius on the test plate list. This change in radii resulted in a change in the performance of the lens systems away from the optimized design. Thus, it was necessary to adjust other parameters to compensate. Using element thicknesses and locations, and the air spacing between the achromatic components, the designs were re-optimized to perform within the specified requirements. This process created a successful design suitable for manufacture (See Figure 12). These same designs were also evaluated for use with a flat window instead of a cylindrical window. Analysis showed that the systems would perform satisfactorily for the flat window as well as the cylindrical window without re-optimization. The next step in the design process was to tolerance the trial lens systems and evaluate their performance.

Tolerance Analysis of the Trial Lens Systems

Zemax offers several features in its tolerance analysis tool that proved to be useful in analyzing the manufactured realization of the trial lens system designs. Tolerances on radius of curvature, element thickness, surface decenters and tilts, element decenters and tilts and surface irregularity were all used in the analysis. In addition, Zemax offers a Monte Carlo analysis feature that computes a total effect of random variance of all the defined tolerance parameters at once.

In preparing to tolerance the systems that had been designed, Specialty Optics Manufacturing and Design, Inc. was again contacted for typical tolerance values that could be held in the manufacture of the trial lens designs. In discussions with their engineers[17], the following tolerances were delineated for quality optics at a reasonable cost:

Radius of Curvature: $\pm$ 1%

Total Instrument Run-out (TIR): 2 minutes of arc (5.8×10^{-4} rad)

Mounting Assembly Decenter: $\pm$ .005 inches (127 μm)

Mounting Assembly Tilt: $\pm$ 8.1 seconds of arc (3.9×10^{-5} rad).

These values were then incorporated into the Zemax tolerance analysis tool, and the effects of these tolerances on the designs was determined. This was accomplished by defining minimum and maximum allowable limits for each of the parameters involved.

The radius of curvature, mounting assembly decenter, and tilt are easily defined tolerances, for their names are descriptive of their effects. TIR, however, refers to a combination of manufacturing errors that culminate in an angular specification. TIR encompasses the effects of relative decentration of surfaces with respect to one another and the effects of improper edging of the lenses.[13]

There were two distinct options in Zemax for tolerancing the systems. The first operation involved the sensitivity of the total system to the specified tolerances of the individual parameters. For radii and thickness tolerances, Zemax accomplished this by modifying the given parameter by the minimum and maximum values and recording the resulting change in performance for both. (Performance changes were referenced to a software-generated merit function similar to the user-defined merit function discussed earlier.) For tolerances on surface decentration, surface tilt and TIR, Zemax modeled each surface as an irregular surface. The shape of this irregular surface was modified from its initial form as a function of the values for the tolerance parameters, spherical aberration, astigmatism, and coma. The same analysis approach was used: minimum and maximum values for each parameter were selected in turn with the resulting change in the merit function recorded for each. Results from this analysis showed that no one parameter was seen to dominate the system performance over its tolerance range when compared to the effects of the other parameters.

The second tolerancing option available in Zemax is a determination of the total effect of the variation of all the toleranced parameters. This is accomplished in Zemax by using a Monte Carlo analysis technique that randomly selects values for each of the tolerance parameters within the specified tolerance range. The normal probability distribution for each parameter was set up so that the tolerance range for the variance of that parameter extended from two standard deviations below zero to two standard deviations above zero.[10] This ensured that a parameter's value occurring outside the specified tolerance range would be a rare event. The result was a lens system whose radii of curvature, thicknesses, decentrations, and tilts modeled a manufactured system based on the trial design. A sample size of one hundred such model systems per design was constructed.

Once these Monte Carlo model systems were completed for each design, the system whose merit function differed the most from its optimal design was selected and examined for performance. This modeled system was then re-optimized by varying only the parameters that would be available to compensate for defects in a manufactured design: the air spacing within each achromatic element, the element locations, and the moving element travel distance. Thus, a determination was made as to whether or not the manufactured systems could be made to perform within the specified requirements and achieve the desired results after manufacture to the specified tolerances. Once this phase was completed with the design and tolerancing of successful trial lens systems, it was necessary to develop a FORTRAN code with which to calculate the propagation of the Gaussian beams to evaluate the beam spot radius at the focal plane.

Up to this point in the design process, all development and analysis was based on a ray approximation to the input laser beams. Though Zemax offers the capability to evaluate Gaussian beam parameters, it is limited to the analysis of rotationally symmetric beam/system combinations.[10] The off-axis nature of the beams and the cylindrical window clearly violate this restriction.

Development of the FORTRAN Code

The FORTRAN code developed to calculate the Gaussian beam spot radius at the focal planes of the optics systems consists of two basic components. The first is a simple, non-paraxial geometric ray trace algorithm, and the second is an algorithm designed to calculate the ABCD matrix parameters of each surface encountered by each of the off-axis beams as they propagate through the system. The ray trace algorithm is used to provide a description of the propagation of the central ray of each Gaussian beam. This, in turn, is used to calculate the required ABCD matrix elements described in Chapter 2.

The basic ray trace algorithm was discussed in Chapter 2. However, due to the presence of cylindrical and flat windows in the optics system, a formulation for calculation of translation and refraction matrices for these surface types had to be made. Using the same approach as Smith[9], translation to a cylindrical surface was accomplished by solving for the translation distance z to a cylinder oriented with its longitudinal axis parallel to the x-axis of the optical system and perpendicular to the optic axis. The curved radius of the cylinder was located in the y-z plane. For this application with off-axis beams, the x-z plane is the tangential plane, and the y-z plane is the sagittal plane. Therefore, the equation for the cylinder is given as

$$\frac{y'^2 + \left[z - \left(d' + R_S\right)\right]^2}{R_S^{\,2}} = 1. \tag{36}$$

Using the expression previously derived by Smith[9]

$$y' = y + \frac{z\beta}{n\cos\theta}, \tag{37}$$

the solution for z can be expressed as

$$z = \frac{(-n\cos\theta)P \mp n\cos\theta\sqrt{P^2 - 4SQ}}{2S}, \tag{38}$$

where

$$P = 2nd'\cos\theta + 2nR_S\cos\theta - 2\beta y \tag{39}$$

$$Q = d' + 2d'R_S + y^2 \tag{40}$$

$$S = \beta^2 + n^2\cos^2\theta, \tag{41}$$

where d' is the distance traveled by the ray to reach the given surface. The sign selection for the square root term in the numerator of the expression for z is determined by the orientation of the given surface. Surfaces with the convex surface facing the negative z-direction are considered as R>0, and would use a negative sign before the square root term. Opposite orientation of the surface would result in the use of the positive sign preceding the square root term. For a flat surface, it is clear that the distance z simply equals the vertex separation distance.

Calculation of the refraction effects at a cylindrical interface was more complicated than that for the effects of translation. Again, using Smith's[9] approach, the vector formulation of Snell's law provided a way to calculate the effects of refraction on the chief ray of the beam. Using the equations

$$n\vec{v} = \begin{bmatrix} n\sin\theta\cos\varphi \\ n\sin\theta\sin\varphi \\ n\cos\theta \end{bmatrix} = \begin{bmatrix} \alpha \\ \beta \\ \sqrt{n^2 - (\alpha^2 + \beta^2)} \end{bmatrix} \tag{42}$$

$$n'\bar{v}' = \begin{bmatrix} n'\sin\theta\cos\varphi \\ n'\sin\theta\sin\varphi \\ n'\cos\theta \end{bmatrix} = \begin{bmatrix} \alpha' \\ \beta' \\ \sqrt{n'^2 - (\alpha'^2 + \beta'^2)} \end{bmatrix} \tag{43}$$

$$\hat{n} = \begin{bmatrix} -x/R \\ -y/R \\ \sqrt{1-(x^2+y^2)/R^2} \end{bmatrix} \tag{44}$$

for the unit vectors of the incident ray ($\bar{v}$), refracted ray ($\bar{v}'$) and inward, unit surface normal ($\hat{n}$), respectively, Snell's law can be expressed as

$$n\bar{v} \times \hat{n} = n'\bar{v}' \times \hat{n}, \tag{45}$$

where n is the index of refraction.

Equating the vector components yields solutions for the slope update equations given by

$$\alpha' = C_x x + \alpha \tag{46}$$

$$\beta' = C_y y + \beta, \tag{47}$$

such that

$$C_x = 0 \tag{48}$$

$$C_y = \frac{P \mp \sqrt{P^2 - Q}}{R_S{}^2} \tag{49}$$

where

$$P = R_S\sqrt{n^2 - \left(\alpha^2 + \beta^2\right)}\sqrt{1 - \frac{y^2}{R_S{}^2}} - \beta y \tag{50}$$

$$Q = R_S^2 \left(n^2 - n'^2\right). \tag{51}$$

Using the ray tracing equations, the expression of the incident angle in the tangential plane of the traced ray at a surface was generated. This equation was easily constructed by analyzing the path of the ray at a surface with a circular cross-section (See Figure 13). The incident angle was expressed as

$$\theta_i = \left|\arctan(\alpha) + \arcsin\left(\frac{x}{R_T}\right)\right|. \tag{52}$$

The second component of the code centers on the determination of the system ABCD matrix. As shown in Chapter 2, this could be accomplished by calculating the refraction matrix at each surface and then cascading the individual ABCD matrices for translation and refraction in the proper order. The code was designed to do this. The equations used were those initially derived by Massey and Siegman[8], as later modified by Siegman[7] to satisfy the normalization property of the ABCD matrix determinant.

The code was written to calculate the refraction matrix of the proper surface element and then matrix multiply it with the corresponding translation matrix. This translation/refraction matrix pair was then matrix multiplied with the previous translation/refraction matrix pair. Following the last surface, the translation/refraction matrix pair was multiplied with the final translation matrix, which described the translation to the focal plane. The result of these calculations was an ABCD matrix that described in detail the total effect of the system on the chief ray of the beam. These matrix values were then used to compute the output beam spot radius using the ABCD transformation law.[7]

In order to calculate the spot radius of the output beam in the tangential and sagittal planes, it was necessary to solve the ABCD transformation law for the complex *q*-parameter in terms of the spot radius. Using equations (19) and (20), the complex *q*-parameter at a defined output plane is given explicitly as

$$\tilde{q}_2 = \frac{-jB\lambda_1 R_1 + B\pi\omega_1^{\,2} + A\pi R_1\omega_1^{\,2}}{-jD\lambda_1 R_1 + D\pi\omega_1^{\,2} + C\pi R_1\omega_1^{\,2}}, \tag{53}$$

noting that $n_1 = n_2 = 1.00$ since input and output values are both calculated in air for this application. (Note: For calculation of the *q*-parameter in the tangential or sagittal plane, the appropriate input values and matrix values for that plane must be used.) Converting this equation into a form that matches the definition of $1/\tilde{q}$ by rationalizing the denominator of the complex fraction gives

$$\begin{aligned}\frac{1}{\tilde{q}_2} = {} & \frac{(\lambda_1 R_1)^2 BD + (\pi\omega_1^{\,2})^2 (D + CR_1) + (B + AR_1)}{(B\lambda_1 R_1)^2 + \left[\pi\omega_1^{\,2}(B + AR_1)\right]^2} \\ & - j\frac{D\lambda_1 R_1 \pi\omega_1^{\,2}(B + AR_1) - B\lambda_1 R_1 \pi\omega_1^{\,2}(D + CR_1)}{(B\lambda_1 R_1)^2 + \left[\pi\omega_1^{\,2}(B + AR_1)\right]^2}.\end{aligned} \tag{54}$$

Equating real and imaginary parts of this equation with the definition of $1/\tilde{q}_2$ given by

$$\frac{1}{\tilde{q}_2} = \frac{1}{R_2} - j\frac{\lambda_2}{\pi\omega_2^2} \tag{55}$$

leads to a solution for the output spot radius given by

$$\omega_2 = \sqrt{\frac{(B\lambda_1 R_1)^2 + \left[\pi\omega_1^2 (B + AR_1)\right]^2}{(R\pi\omega_1)^2 (AD - BC)}} . \tag{56}$$

Thus, using the system ABCD matrix calculated previously, it was possible to determine the output spot radius of the off-axis input beam given knowledge of the input spot radius, phase curvature, and wavelength.

Chapter 4

Results

Optical Systems Obtained

Completion of the design of the focusing optics resulted in two optimized trial lens systems for each representative duct size: one in-line system and one folded system. All ten designs consisted of two air-spaced achromatic elements with manufacturable radii and thicknesses. Explicit descriptions for each of the trial lens systems, including lens radii of curvature, lens thicknesses, air spacings, and element travel distances are included in Appendix B, Trial Lens Systems for RELIEF Focusing Optics.

FORTRAN Code Validation

Validation of the FORTRAN code was necessary before analysis of the trial lens systems for Gaussian beam focusing could take place. The output spot radii from the FORTRAN code were validated by comparing them with similar Gaussian beam data from Zemax for several rotationally symmetric systems, including some containing large amounts of spherical aberration. (The rotational symmetry was required by Zemax and not the FORTRAN code.[10]) These systems were generated by employing modified versions of the designs previously completed in this thesis. A flat window and an on-axis beam were used in order to create the required rotational symmetry for Zemax. The input beam parameters (shown in Table 1) were calculated for a beam that had

Table 1. Input Beam Parameters

		532 nm	532 nm	580 nm	580 nm
System	Beam Waist (mm)	Spot Radius (mm)	Phase Curvature	Spot Radius (mm)	Phase Curvature
4 Inch	0.75	1.01	6.70 m	1.05	6.10 m
1 Foot	1.10	1.19	20.0 m	1.21	17.3 m
3 Feet	2.50	2.51	475.0 m	2.51	386.1 m
6 Feet	5.00	5.00	7.265 km	5.00	7.265 km
12 Feet	7.50	7.50	36.789 km	7.50	36.789 km

propagated a distance a distance of three meters from its waist before reaching the focusing optics. The spot radii results are given in Table 2, and they show a maximum difference of less than 5% between the FORTRAN code and Zemax. Thus, the code was shown to be valid in this limited application.

Beam Spot Radii Results

Following validation of the FORTRAN code for on-axis beams, each of the optimized trial lens systems was evaluated for use with an off-axis beam and a cylindrical window. Additionally, these systems were evaluated for performance with a flat window to account for potential manufacturing or cost-restrictive difficulties with the cylindrical window. The input beam parameters were the same as those described above. Table 3 shows the results of the analysis for the cylindrical window, and Table 4 shows the results of the same systems employing a flat window. (Only a change in the results in the sagittal plane occurred since the infinite radius of curvature of the window occurs in the tangential plane of the optics.)

Table 2. Comparison of spot radii calculated by FORTRAN code and Zemax for rotationally symmetric systems.

	Far Focus				Near Focus			
	FORTRAN Code Spot Size (μm)		Zemax Spot Size (μm)		FORTRAN Code Spot Size (μm)		Zemax Spot Size (μm)	
System	532 nm	580 nm	532 nm	580 nm	532 nm	580 nm	532 nm	580 nm
Inline-4 In	16.87	18.40	16.70	18.30	13.40	14.60	13.30	14.51
Folded-4 In	31.18	33.68	30.95	33.54	25.48	27.42	25.55	27.34
Inline-1 Ft	31.25	34.01	31.17	33.98	20.89	22.60	20.79	22.57
Folded-1 Ft	36.09	39.28	36.08	39.27	24.92	27.10	24.85	27.05
Inline-3 Ft	39.07	42.37	39.13	42.56	26.99	28.35	27.33	28.78
Folded-3 Ft	45.65	49.79	45.44	49.58	31.30	33.83	31.03	33.64
Inline-6 Ft	47.45	50.31	47.96	50.14	26.85	28.41	26.66	28.56
Folded-6 Ft	42.64	46.47	42.69	46.49	30.12	32.32	29.91	32.25
Inline-12 Ft	80.35	83.10	83.91	83.91	40.45	41.95	39.32	41.71
Folded-12Ft	61.29	66.29	61.90	66.47	46.39	49.01	45.69	48.75

Table 3. Orthogonal Beam Parameters at the focus through a Cylindrical Window for Optimized Trial Lens Systems.

	Far Focus				Near Focus			
	Spot Size (μm) Tangential		Spot Size (μm) Sagittal		Spot Size (μm) Tangential		Spot Size (μm) Sagittal	
System	532 nm	580 nm	532 nm	580 nm	532 nm	580 nm	532 nm	580 nm
Inline-4 In	13.60	14.70	21.00	21.00	8.46	8.22	8.26	8.65
Folded-4 In	25.10	25.10	17.90	18.10	24.70	24.90	10.50	11.30
Inline-1 Ft	29.00	30.70	38.00	47.50	18.70	23.70	15.60	18.10
Folded-1 Ft	34.60	35.30	37.80	47.00	21.90	24.00	21.50	23.10
Inline-3 Ft	48.50	50.60	45.60	48.10	46.80	47.20	18.40	20.00
Folded-3 Ft	45.10	49.20	49.70	53.20	35.60	37.40	28.00	30.60
Inline-6 Ft	48.90	51.80	49.10	51.90	51.70	52.50	21.10	22.90
Folded-6 Ft	42.30	46.10	49.00	52.30	41.00	42.50	26.50	28.90
Inline-12 Ft	87.50	90.10	57.20	61.00	98.70	99.20	25.60	27.80
Folded-12Ft	59.70	64.80	61.70	66.60	81.50	82.90	36.00	39.30

Table 4. Orthogonal Beam Parameters at the focus through a Flat Window for Optimized Trial Lens Systems.

	Far Focus				Near Focus			
	Spot Size (µm) Tangential		Spot Size (µm) Sagittal		Spot Size (µm) Tangential		Spot Size (µm) Sagittal	
System	532 nm	580 nm	532 nm	580 nm	532 nm	580 nm	532 nm	580 nm
Inline-4 In	13.60	14.70	16.20	17.60	8.46	8.22	11.40	12.20
Folded-4 In	25.10	25.10	19.50	21.20	24.70	24.90	13.80	15.00
Inline-1 Ft	29.00	30.70	30.70	30.60	18.70	23.70	17.20	17.10
Folded-1 Ft	34.60	35.30	35.70	35.40	21.90	24.00	23.60	23.40
Inline-3 Ft	48.50	50.60	36.60	39.90	46.80	47.20	18.50	20.20
Folded-3 Ft	45.10	49.20	45.40	49.50	35.60	37.40	28.50	31.10
Inline-6 Ft	48.90	51.80	39.10	42.60	51.70	52.50	21.00	23.00
Folded-6 Ft	42.30	46.10	42.50	46.30	41.00	42.50	26.70	29.10
Inline-12 Ft	87.60	90.10	49.80	54.20	98.70	99.20	25.60	27.80
Folded-12Ft	59.70	64.80	58.10	63.40	81.50	82.90	36.10	39.40

Since the beams were acted upon differently in the tangential and sagittal planes, elliptical spots rather than circular spots were created at the focal planes. Thus, when analyzing the output, it was necessary to evaluate the area of the spot in order to determine true performance. The elliptical spots resulted from astigmatism caused by the beams passing off-axis through the optics and by the cylindrical window. Under normal circumstances, this astigmatism could be minimized by employing defocus and locating the circle of least confusion at the focal plane. An attempt to do just this was made using the through-focus spot diagram tool in Zemax. This tool clearly showed the effects of astigmatism on the beam and allowed location of an image plane close to the circle of least confusion. Defocusing the image plane of the optics to the location of this plane near the circle of least confusion resulted in a smaller, more circular spot, but the two beams were no longer co-located as required for this RELIEF technique. Thus, the defocusing adjustment could not be used.

Comparison of the results for the cylindrical window versus the flat window indicates a slightly better performance in terms of output spot area in the far focus by using the flat window, since the flat window produced smaller spot radii in the sagittal plane of the optics. However, it is not clear how the flat window would affect the airflow inside the duct. Either the window would protrude into the duct, or it would create a recess. In either case it may prove necessary to incorporate fairings before and after the window to reduce any turbulence generated by use of a flat window.

The final evaluation necessary to determine the feasibility of these focusing optics was assessment of the results for the Monte Carlo trials, which modeled manufactured optics. Monte Carlo analysis for each of the optimized trial lens systems resulted in one hundred models of manufactured designs. For each system, the model that differed most from its corresponding optimized system was selected and analyzed. Performance of these models within the established requirements was obtained through optimization using only those parameters available after manufacturing. The same input beam parameters were used as for the optimized trial lens systems, and the results are given in Table 5. Analysis of this data for the beam spot radii shows the ability of nearly all of the manufactured models to perform within the established requirements. This achievement shows the feasibility of the focusing optics in terms of simulated, post-manufacture performance. In addition, with the tolerance parameters that were included in the analysis, it is probable that these focusing systems will be able to perform adequately in the test cell environment in terms of vibration.

The models for the four inch, and one, three, and six foot ducts, produced output spot areas smaller than that required in both the near and far focal planes. The designs for the twelve foot diameter ducts showed the worst performance of all the designs in terms of meeting the output spot radius criteria at the focal plane. The spot area for each of the beams was 65% to 80% larger in the far focus and 30% to 40% larger in the near focus than the area for a spot with a 50 μm radius currently used in RELIEF tagging. However, this increase in focused spot area can be accounted for with a corresponding per pulse energy increase. The laser being used for development of this RELIEF technique should provide up to approximately 160 mJ per pulse at 532 nm and 64 mJ at 580 nm. The

Table 5. Orthogonal Beam Properties at the focus through a Cylindrical Window for Models of Manufactured Systems.

	Far Focus				Near Focus			
	Spot Size (μm) Tangential		Spot Size (μm) Sagittal		Spot Size (μm) Tangential		Spot Size (μm) Sagittal	
System	532 nm	580 nm	532 nm	580 nm	532 nm	580 nm	532 nm	580 nm
Inline-4 In	14.70	16.00	29.90	20.90	8.67	9.18	8.48	8.96
Folded-4 In	24.30	24.30	17.90	18.00	28.40	28.60	10.60	10.90
Inline-1 Ft	29.20	31.60	37.80	47.30	19.40	24.30	15.70	18.40
Folded-1 Ft	32.90	34.60	38.20	47.70	27.30	24.50	27.80	24.70
Inline-3 Ft	46.50	48.80	42.40	46.80	46.00	46.40	18.90	20.60
Folded-3 Ft	46.20	50.30	50.40	54.00	34.00	36.00	28.50	31.10
Inline-6 Ft	50.00	52.90	44.30	47.50	52.30	53.10	21.70	23.60
Folded-6 Ft	42.70	46.40	51.10	54.20	42.90	44.30	26.00	28.30
Inline-12 Ft	83.70	86.40	53.90	58.00	98.20	98.70	25.60	27.80
Folded-12Ft	59.10	64.40	69.40	73.90	85.90	87.30	37.00	40.30

energy requirements for the two configurations for the twelve foot ducts are shown in Table 6, along with the available per pulse energy for each wavelength from the laser being used in the development of this RELIEF technique. Clearly, the results show that RELIEF tagging is possible with the folded configuration. The inline configuration requires 4.2% more energy in the far focus for the 580 nm beam than the laser is predicted to provide. However, it is very likely that this small increase can be achieved with further optimization of the optics once a final design for the entire RELIEF systems is established.

Co-location of the two off-axis beams was evaluated using the spot diagram tool in Zemax. The diagram was referenced to the chief ray of each beam and showed a separation of no more than 1 to 2 microns for all of the trial lens systems designs. This separation is small when compared to the spot area generated by the two co-located beams.

The overall lengths of the inline systems were within 15% of the representative value of one half the duct radius except for the four inch duct, which was 53% longer than required, corresponding to an extra 39 mm in the overall length. However, this extra length was necessary to achieve the co-location of the beams and the required spot radii at focus. This small increase should not result in any difficulties since the space available for the optics is not as restrictive for the four inch duct as for the other ducts.

Table 6. Per Pulse Energy Requirements and Available Per Pulse Energy for Trial Lens System Designs for the Twelve Foot Duct

	Far Focus		Near Focus	
	532 nm	580 nm	532 nm	580 nm
12 Ft-Inline	120 mJ	66.7 mJ	67.0 mJ	36.6 mJ
12 Ft-Folded	109 mJ	63.4 mJ	84.8 mJ	46.9 mJ
Energy Available	160 mJ	64 mJ	160 mJ	64 mJ

Chapter 5

Conclusion

Summary of Results

Successful trial lens system designs for focusing optics for the use of RELIEF in engine test facilities were generated using the Zemax optical design program. The systems were obtained using ray approximations to the input beams for which the spot size at the focus was minimized about the chief ray and for which the two beams were co-located at the focal plane of the optics. Each of these systems met the established requirements for beam co-location, and with the Nd:YAG laser being used in development of this point-tagging RELIEF technique, an achievable per pulse energy increase will ensure successful RELIEF tagging performance for each duct. In terms of meeting the overall length constraint, all the trial lens systems were within an acceptable margin of the initial goal, accounting for the unique restrictions of each duct size.

Also, due to Zemax's inability to calculate reliable Gaussian beam data for non-rotationally symmetric systems, a FORTRAN code was developed to perform the analysis of the focused spot radii of the two off-axis Gaussian laser beams. This code was validated by comparing Gaussian beam data obtained for rotationally symmetric systems to similar data obtained using Zemax, including some containing large amounts of spherical aberration. The results showed a maximum 5% difference.

Further Considerations

Further investigation into the correction of the astigmatism generated by the off-axis nature of the beams and the cylindrical window would be advisable. Several methods, such as cylindrical optics with rotated and inverted orientations, with respect to the access window, were investigated during the course of this thesis, but none significantly reduced the astigmatism.

Also, since the input laser beams are likely to propagate a long distance before reaching the focusing optics, it would be advisable to consider optical systems whose lens diameters are much larger than that simply required to provide a suitable tagged point in the flow. These larger diameters would decrease potential vignetting of the beams due to vibration of the focusing optics or to misalignment of the optics directing the input beams to the focusing optics. Though vibration was considered in terms of maintaining a focused spot with co-located beams, this aspect still requires consideration.

Utilizing a thermal analysis feature available in Zemax (v. 4.5) that models the effects of temperature and pressure on the index of refraction, radius of curvature, thickness, and parameter 1 values (which are surface-type dependent) for each element of a given lens system should be another aspect of future work. However, at the time of this writing, this thermal analysis feature may not give accurate results for decentered systems.[10]

An additional recommendation for future work would be to re-check the accuracy of the FORTRAN code by using software scheduled for release in the near future that will be able to calculate Gaussian beam parameters for off-axis beams such as those utilized in the RELIEF technique discussed in this thesis.

Implications for RELIEF

The feasibility of focusing optics for the use of RELIEF in engine test facilities has been quantitatively shown in this thesis. Additionally, a design methodology and means of performance analysis for these optics has been presented. The capabilities of Zemax have been shown to be adequate as a design tool for this application, and the performance of the FORTRAN code has been shown to effectively predict the spot radii at the focal plane in this limited case of small, off-axis beams. Further development of these focusing optics are contingent on several factors.

First, the optics that will image the tagged flow must be shown to be feasible. Second, an engineering concept outlining the RELIEF system setup in each test cell, including the precise amount of space available to mount the focusing optics outside the engine-inlet duct, must be developed. Finally, the optics that will deliver the two laser beams to the focusing optics must be designed. Once these steps are completed, the design methodology and analysis procedures outlined can be used to revise the focusing optics designs presented in this thesis to account for any changes associated with the final design of the RELIEF system.

References

1. E. C. Markovitz, *Measurements of Turbulence Qualities in the Near Field of an Underexpanded Sonic Jet by Raman Excitation and Laser-Induced Electronic Fluorescence*, Master's Thesis, Princeton University, 1988.

2. W. R. Lempert, et. al., "Subsonic Flow Vector Measurement by RELIEF Flow Tagging," SBIR Presentation Meeting at AEDC, October 1995.

3. W. R. Lempert, et. al., "Stimulated Raman scattering and coherent anti-Stokes Raman spectroscopy in high-pressure oxygen," J. Opt. Soc. Am. B **7**, 1990.

4. R. B. Miles, et. al., "Fundamental Turbulence Measurements by Relief Flow Tagging," AIAA Journal **31**, 1993.

5. B. Zhang, W. R. Lempert and R. B. Miles, "Efficient vibrational Raman conversion in O2 and N2 cells by use of superfluorescence seeding," Optics Letters **18,** 1993.

6. R. B. Miles, et. al., "Instantaneous supersonic velocity profiles in an underexpanded sonic air jet by oxygen flow tagging," Phys. Fluids A **1**, 1989.

7. A. E. Siegman, *LASERS* (Univ. Sci. Books, Mill Valley, 1986).

8. G. A. Massey and A. E. Siegman, "Reflection and Refraction of Gaussian Light Beams at Tilted Ellipsoidal Surfaces," Appl. Opt. **8**, 1969.

9. L. M. Smith, *Fundamental Principles of Optical Engineering* (Univ. of Tenn. Space Inst., Tullahoma, 1993).

10. Zemax Optical Design Program User's Guide, Version 4.5, Tucson, 1990-1995.

11. W. H. Steier, "The Ray Packet Equivalent of a Gaussian Light Beam," Appl. Opt. **5**, 1966.

12. W. J. Smith, *Modern Optical Engineering, The Design of Optical Systems* (McGraw-Hill, Inc., New York, 1990).

13. P. R. Yoder, Jr., *Opto-Mechanical Systems Design* (Marcel Dekker, Inc., New York, 1993).

14. A. R. Mickelson, *Physical Optics* (Van Nostrand Reinhold, New York, 1992).

15. Melles Griot Inc., 1995/96 Catalog, USA, 1995.

16. Newport Corporation, *The Newport Catalog 94/95*, USA, 1994.

17. Specialty Optics Manufacturing and Design.

Appendices

Appendix A

Figures

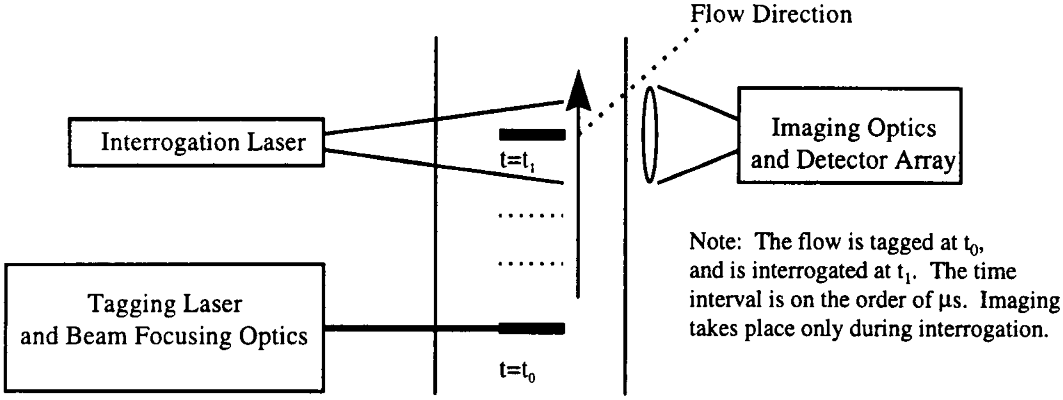

Figure 1. RELIEF Schematic for Tagging and Interrogation of a Line

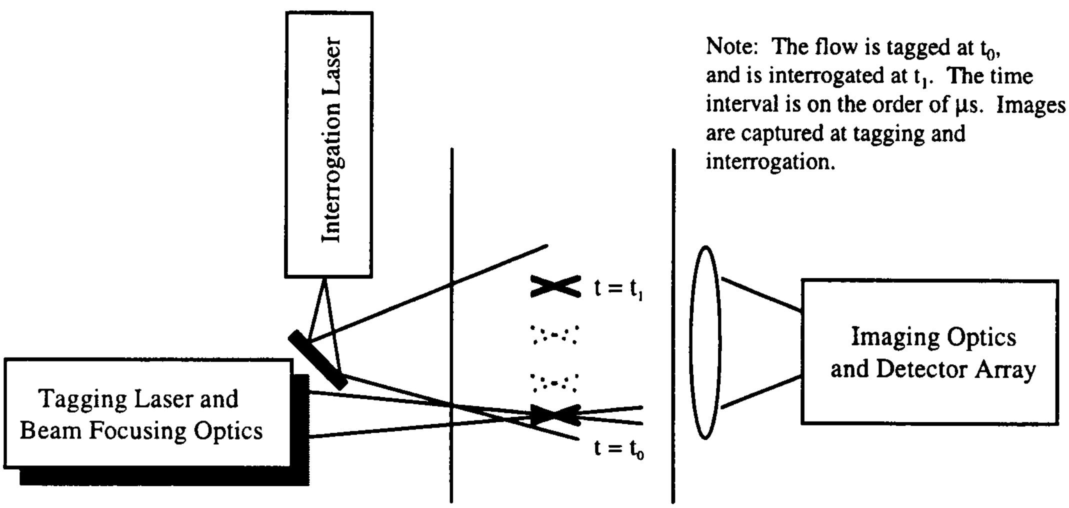

Figure 2. RELIEF Schematic for Tagging and Interrogation of a Point

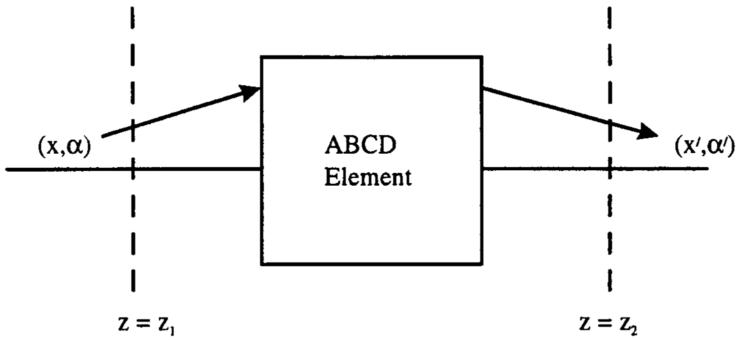

Figure 3. ABCD Optical Element

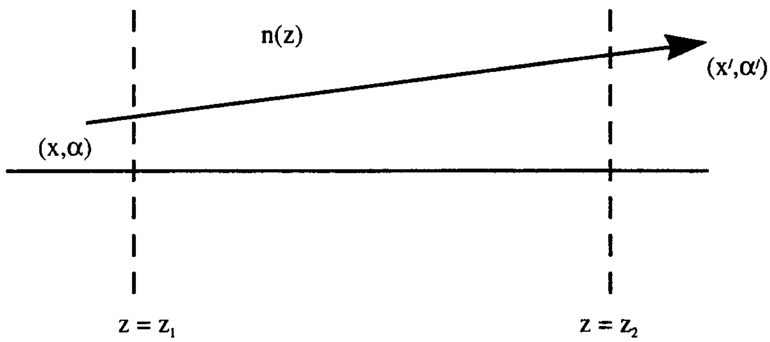

Figure 4. Translation in medium with index of refraction n(z).

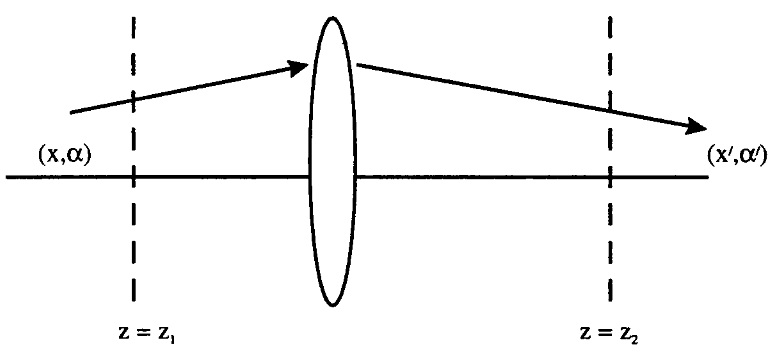

Figure 5. Thin Lens ray transformation.

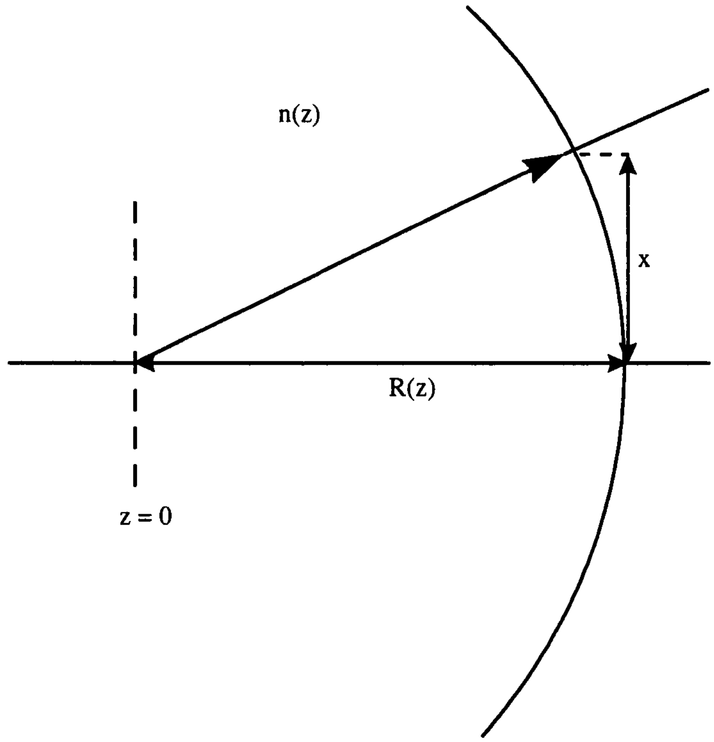

Figure 6. Geometry for Treating Spherical Waves

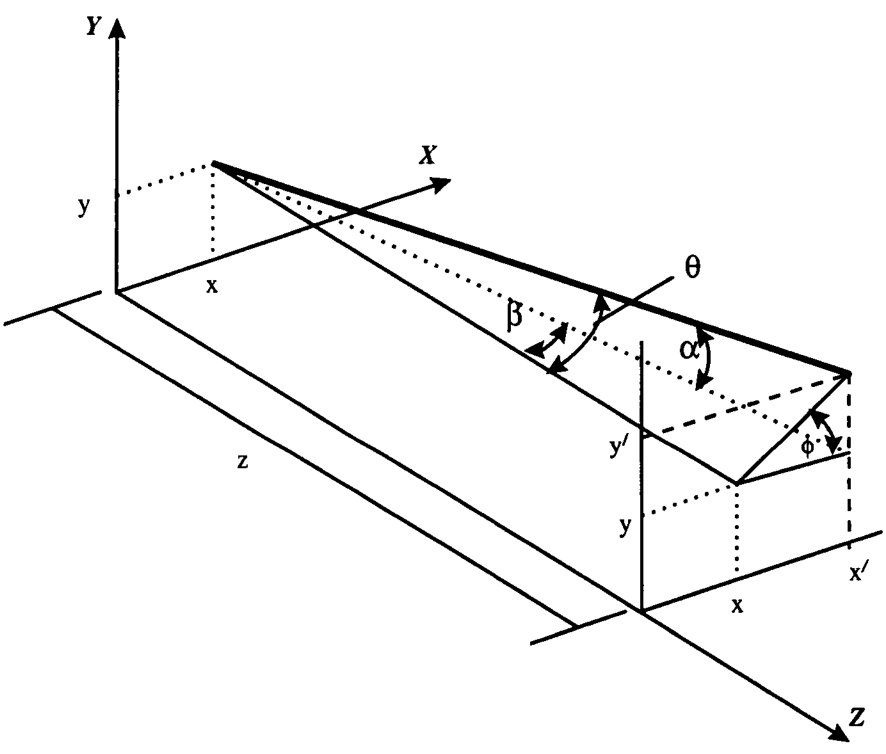

Figure 7. Theta as a Function of α and β in index of refraction n.

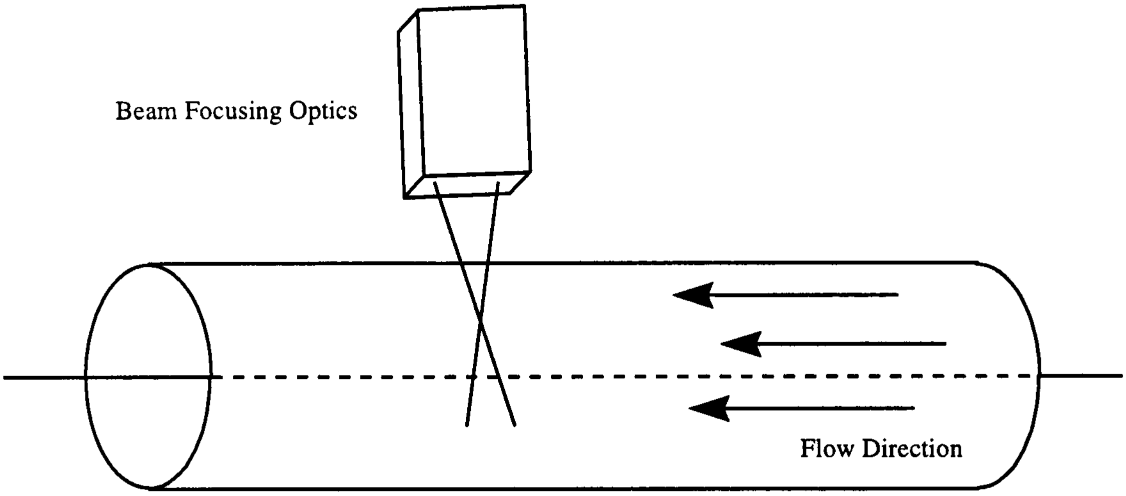

Figure 8. Focusing Optics--Inline Configuration

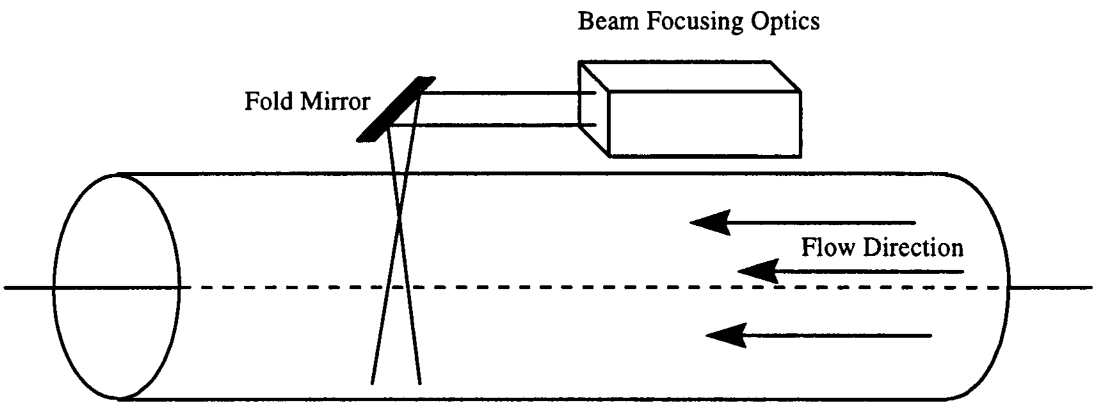

Figure 9. Focusing Optics--Folded Configuration

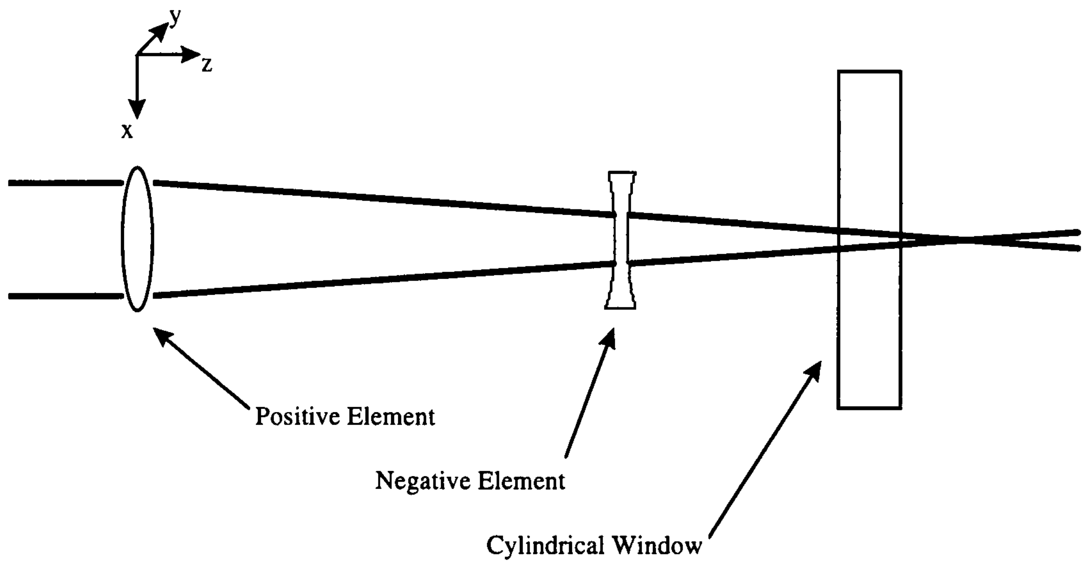

Figure 10. RELIEF Setup for Point Tagging (Near FocusPosition)

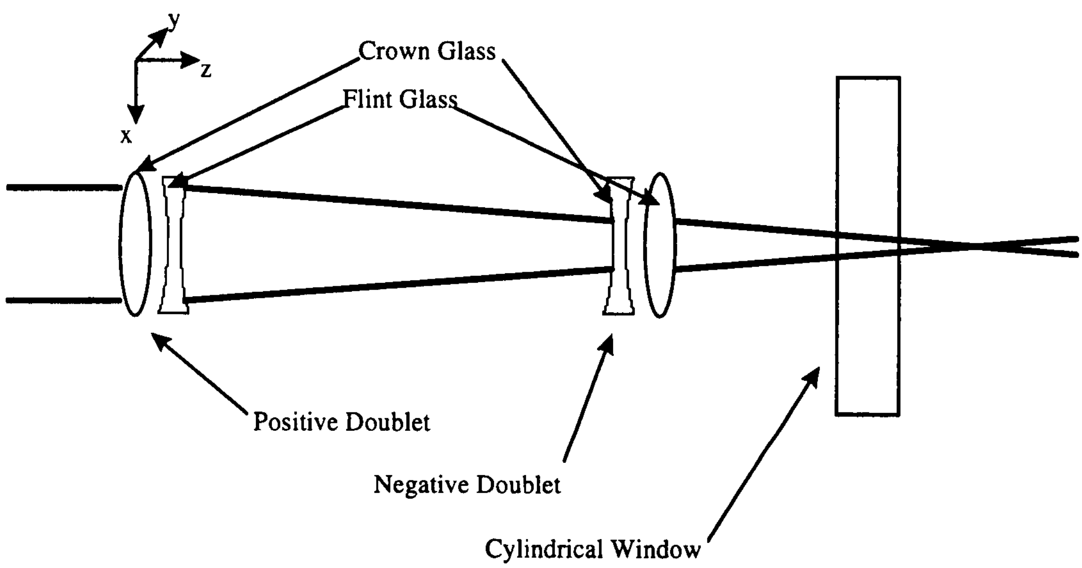

Figure 11. RELIEF Setup for Point Tagging using Achromatic Doublets (Near Focus Position)

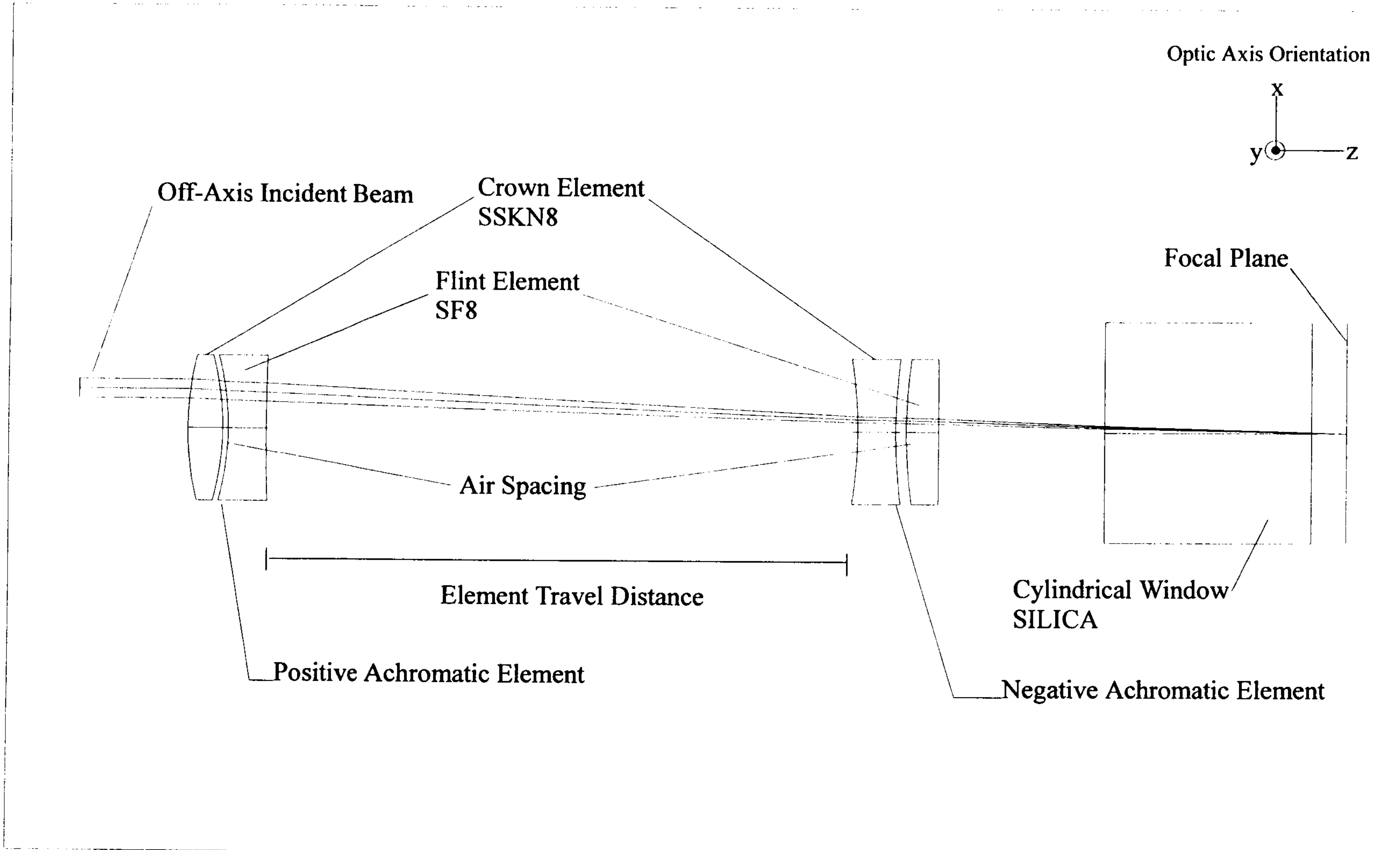

Figure 12. General Schematic of Trial Lens Systems for RELIEF Focusing Optics

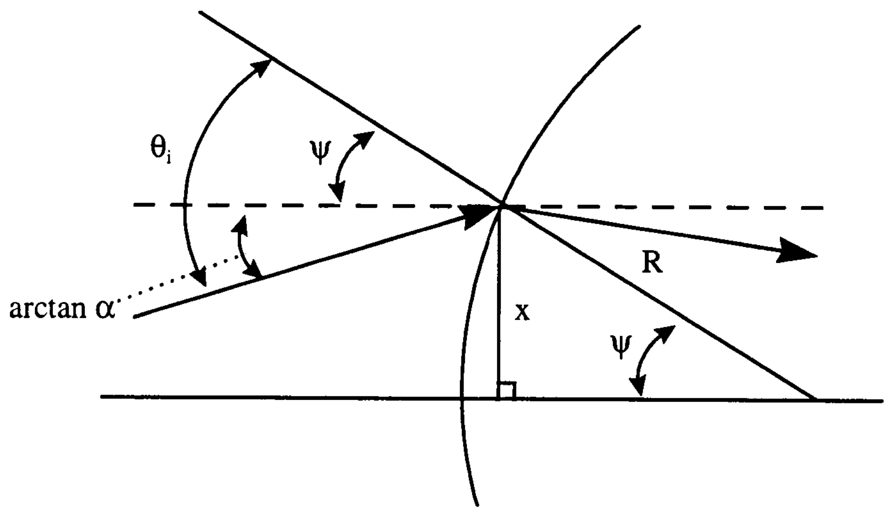

Figure13. Geometry for measurement of incident angle at a circular cross-section.

Appendix B

Trial Lens Systems for RELIEF Focusing Optics

Table B-1: Trial Lens System Parameters—4 In. Duct, Inline Configuration

Surface	Radius (mm)	Thickness (mm)	Glass Type	Diameter (mm)
1	19.11	1.70	SSKN8	10.4
2	-18.23	.527	AIR	10.4
3	-17.39	1.85	SF8	10.4
4	128.3	2.00	AIR	10.4
5	-60.17	1.00	SSKN8	10.4
6	32.18	.306	AIR	10.4
7	44.21	2.00	SF8	10.4
8	-264.9	5.75	AIR	10.4
9	57.15	6.35	SILICA	12.7
10	50.8	---	AIR	12.7
Travel Distance (mm)	23.6			

Table B-2: Trial Lens System Parameters—4 In. Duct, Folded Configuration

Surface	Radius (mm)	Thickness (mm)	Glass Type	Diameter (mm)
1	19.34	1.50	SSKN8	10.4
2	-19.34	.591	AIR	10.4
3	-20.42	2.00	SF8	10.4
4	66.37	2.00	AIR	10.4
5	-39.89	1.00	SSKN8	10.4
6	34.74	1.31	AIR	10.4
7	56.59	2.00	SF8	10.4
8	-83.99	18.8	AIR	10.4
9	57.15	6.35	SILICA	12.7
10	50.8	---	AIR	12.7
Travel Distance (mm)	17.5			

Table B-3: Trial Lens System Parameters—1 Ft. Duct, Inline Configuration

Surface	Radius (mm)	Thickness (mm)	Glass Type	Diameter (mm)
1	43.12	3.20	SSKN8	16.7
2	-39.52	.500	AIR	16.7
3	-41.07	3.50	SF8	16.7
4	277.00	2.00	AIR	16.7
5	-63.98	3.5	SSKN8	16.7
6	82.26	.950	AIR	16.7
7	70.76	3.00	SF8	16.7
8	-1189.11	15.24	AIR	16.7
9	171.45	19.05	SILICA	25.4
10	152.4	---	AIR	25.4
Travel Distance (mm)	52.44			

Table B-4: Trial Lens System Parameters—1 Ft. Duct, Folded Configuration

Surface	Radius (mm)	Thickness (mm)	Glass Type	Diameter (mm)
1	51.66	5.00	SSKN8	16.7
2	-53.6	.862	AIR	16.7
3	-53.6	2.00	SF8	16.7
4	247.21	2.00	AIR	16.7
5	-124.8	2.00	SSKN8	16.7
6	94.37	.236	AIR	16.7
7	101.81	2.00	SF8	16.7
8	-2203.40	44.45	AIR	16.7
9	171.45	19.05	SILICA	25.4
10	152.4	---	AIR	25.4
Travel Distance (mm)	59.98			

Table B-5: Trial Lens System Parameters—3 Ft. Duct, Inline Configuration

Surface	Radius (mm)	Thickness (mm)	Glass Type	Diameter (mm)
1	133.13	10.5	SSKN8	44.10
2	-128.58	.845	AIR	44.10
3	-138.02	8.00	SF8	44.10
4	1540.31	2.00	AIR	44.10
5	-356.22	8.00	SSKN8	44.10
6	164.64	.762	AIR	44.10
7	237.51	8.00	SF8	44.10
8	-4038.39	25.4	AIR	44.10
9	476.25	19.05	SILICA	76.2
10	457.2	---	AIR	76.2
Travel Distance (mm)	180.88			

Table B-6: Trial Lens System Parameters—3 Ft. Duct, Folded Configuration

Surface	Radius (mm)	Thickness (mm)	Glass Type	Diameter (mm)
1	134.29	9.5	SSKN8	44.10
2	-154.12	1.39	AIR	44.10
3	-156.01	10.00	SF8	44.10
4	600.72	2.00	AIR	44.10
5	-330.14	7.00	SSKN8	44.10
6	220.82	5.85	AIR	44.10
7	321.71	10.50	SF8	44.10
8	-1003.00	152.4	AIR	44.10
9	476.25	19.05	SILICA	76.2
10	457.2	---	AIR	76.2
Travel Distance (mm)	156.4			

Table B-7: Trial Lens System Parameters—6 Ft. Duct, Inline Configuration

Surface	Radius (mm)	Thickness (mm)	Glass Type	Diameter (mm)
1	216.04	12.9	SSKN8	76.2
2	-235.59	4.57	AIR	76.2
3	-228.60	7.30	SF8	76.2
4	1111.18	2.00	AIR	76.2
5	-592.822	10.00	SSKN8	76.2
6	307.62	5.00	AIR	76.2
7	820.72	10.00	SF8	76.2
8	-667.44	152.08	AIR	76.2
9	933.45	19.05	SILICA	152.4
10	914.40	---	AIR	152.4
Travel Distance (mm)	325.86			

Table B-8: Trial Lens System Parameters—6 Ft. Duct, Folded Configuration

Surface	Radius (mm)	Thickness (mm)	Glass Type	Diameter (mm)
1	287.90	10.00	SSKN8	76.2
2	-291.23	.862	AIR	76.2
3	-300.85	12.50	SF8	76.2
4	1729.20	2.00	AIR	76.2
5	-646.07	15.50	SSKN8	76.2
6	500.65	5.34	AIR	76.2
7	544.14	12.70	SF8	76.2
8	-7954.29	274.6	AIR	76.2
9	933.45	19.05	SILICA	152.4
10	914.4	---	AIR	152.4
Travel Distance (mm)	356.00			

Table B-9: Trial Lens System Parameters—12 Ft. Duct, Inline Configuration

Surface	Radius (mm)	Thickness (mm)	Glass Type	Diameter (mm)
1	378.61	30.00	SSKN8	164.4
2	-574.15	3.63	AIR	164.4
3	-551.04	30.00	SF8	164.4
4	1346.44	30.00	AIR	164.4
5	-1002.66	24.00	SSKN8	164.4
6	646.07	5.15	AIR	164.4
7	1346.44	35.5	SF8	164.4
8	-1476.59	124.39	AIR	164.4
9	1847.85	19.05	SILICA	304.8
10	1828.8	---	AIR	304.8
Travel Distance (mm)	742.81			

Table B-10: Trial Lens System Parameters—12 Ft. Duct, Folded Configuration

Surface	Radius (mm)	Thickness (mm)	Glass Type	Diameter (mm)
1	528.70	30.00	SSKN8	164.4
2	-645.85	5.68	AIR	164.4
3	-646.07	30.00	SF8	164.4
4	2203.04	30.00	AIR	164.4
5	-1043.00	25.00	SSKN8	164.4
6	1189.106	3.49	AIR	164.4
7	1346.44	25.00	SF8	164.4
8	-3838.85	530.00	AIR	164.4
9	1847.85	19.05	SILICA	304.8
10	1828.80	---	AIR	304.8
Travel Distance (mm)	723.5			

VITA

Carvil Eugene Thomas Chalk was born in Augusta, Georgia on April 27, 1973. He attended a private Christian school until age 9 when his family moved to Cleveland, Georgia where he attended public schools in the White County School system. He graduated from White County High School in May, 1990. In September of 1990 Carvil entered North Georgia College from which he received a Bachelor of Science degree in physics in June of 1994. He entered the graduate program at the University of Tennessee Space Institute, Tullahoma in August of 1994, officially receiving the Master of Science degree in engineering science and mechanics in August of 1996. Carvil worked as a graduate research assistant with Sverdrup Technology, Inc. during his graduate program.